Electronic Supplementary Materials (ESI)

Origin of Heterogeneous Dynamics in Local Molecular Structures for Ionic Liquids

Maolin Sha,*, [a] Yusheng Liu,[b] Huaze Dong,[a] Fabao Luo,[a] Fangling Jiang,[c] Zhongfeng Tang,[c]

Guanglai Zhu,[d] and Guozhong Wu *, [c]

[a] Department of Chemistry and Chemical Engineering, Hefei Normal University, Hefei 230061, China

[b] Department of Chemistry and Chemical Engineering, Xuzhou Institute of Technology, Xuzhou 221000, China

[c] Shanghai Institute of Applied Physics, Chinese Academy of Sciences, Shanghai 201800, P.B. Box 800-204, China

[d] Institute of Atomic and Molecular Physics, Anhui Normal University, Wuhu 241000, China

* E-mail: wuguozhong@sinap.ac.cn;franksha@aliyun.com

1. The densities of $BmimBF_4$ as a function of temperature.

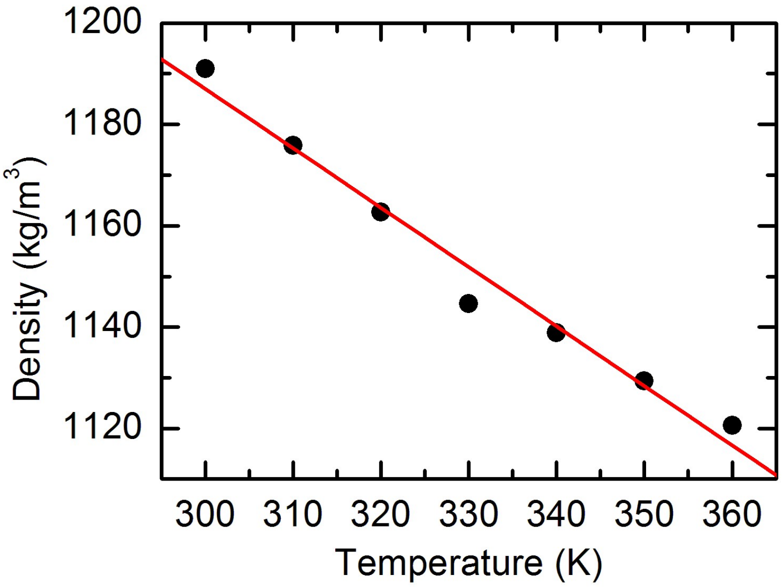

Figure S1. The densities of $BmimBF_4$ as a function of temperature.

We have calculated the density changes of the IL $BMIMBF_4$ as the function of temperature. It was shown in figure S1. Obviously, the densities slightly decreases in a linear trend with the increasing temperature. The calculated density value at 300 K is about 1.19 g/cm^3, which is very close to the experimental value 1.21g/cm^3, indicating a reliable force field parameters of our simulation.

2. The static and dynamics properties of IL $BmimBF_4$ in our simulation at 300 K

Table S1 Static and dynamic properties derived from our MD simulations at 300 K.

Diffusion coefficients (10^{-7} $cm^2.s^{-1}$)		Liquid properties	
Cation	Anion	Density($g.cm^{-3}$)	Viscosity(cP)
1.2(1.8[1],1.2[1])	1.1(1.8[1],1.2[1])	1.19 (1.21[1],1.20[1])	95.3(75.3[1], 100.0[1])

Values in parenthesis are corresponding experimental values available in the cited literature. The first value in the parenthesis is measured at 303.15K where the latter value is measured at 298.15K.

3. The snapshot of polar region and apolar region

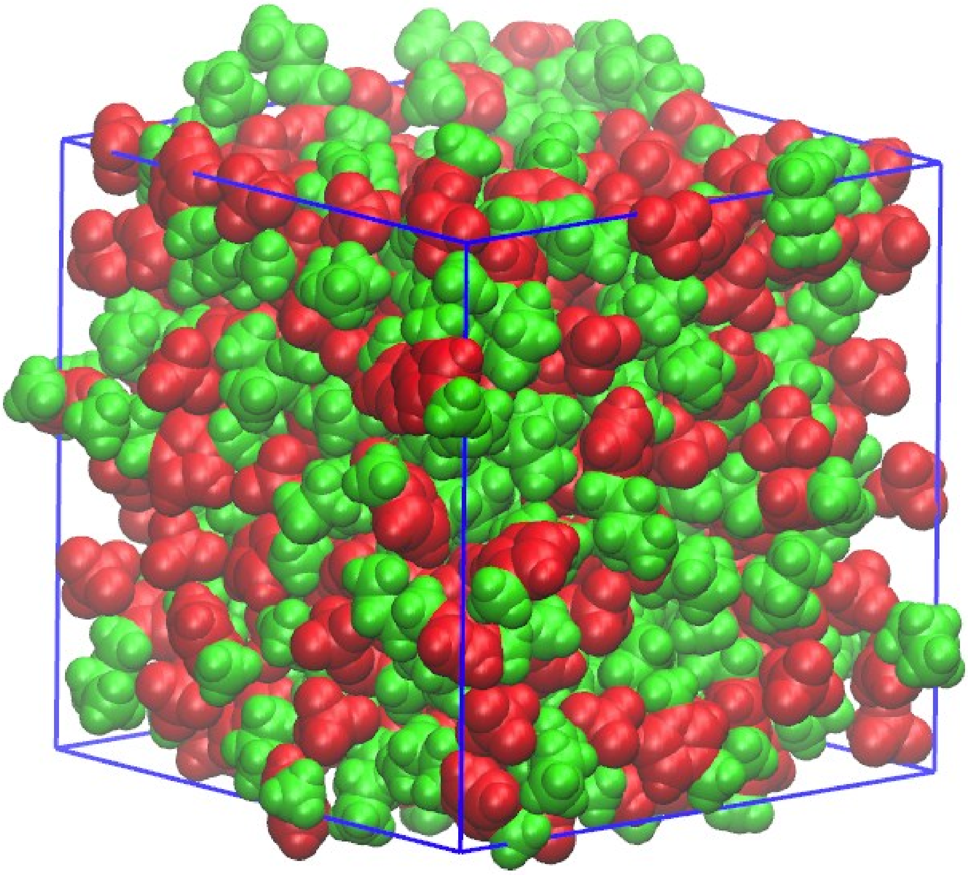

Figure S2. The snapshot of polar region and apolar region at 300K. Polar region including imidazolium ring and anion, was displayed in red color; the apolar region including butyl chain and methyl group, was displayed in green.

4. The radial distribution functions of polar sites and apolar sites

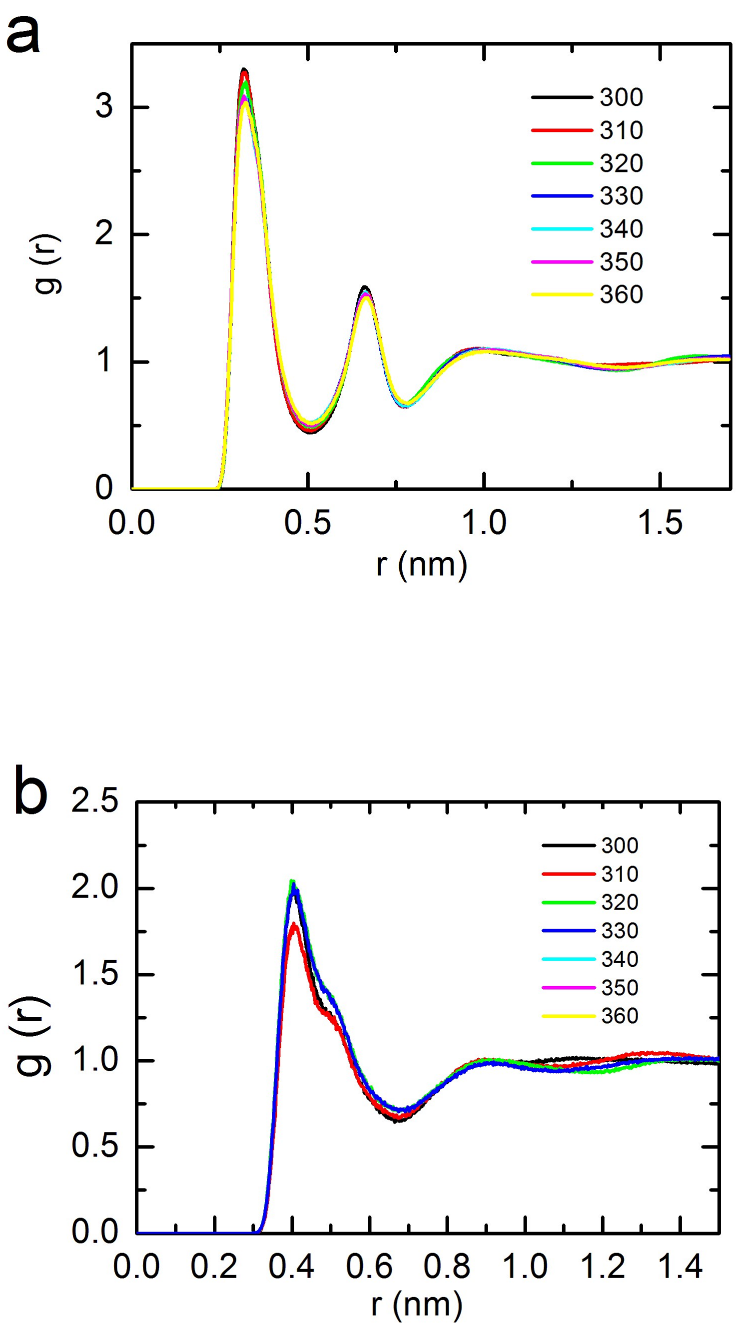

Figure S3 The site-to-site radial distribution functions of polar sites and apolar sites. (a). HA1 (imidazxolium ring)-B (anion). (b). CT4-CT4 (butyl chain ending).

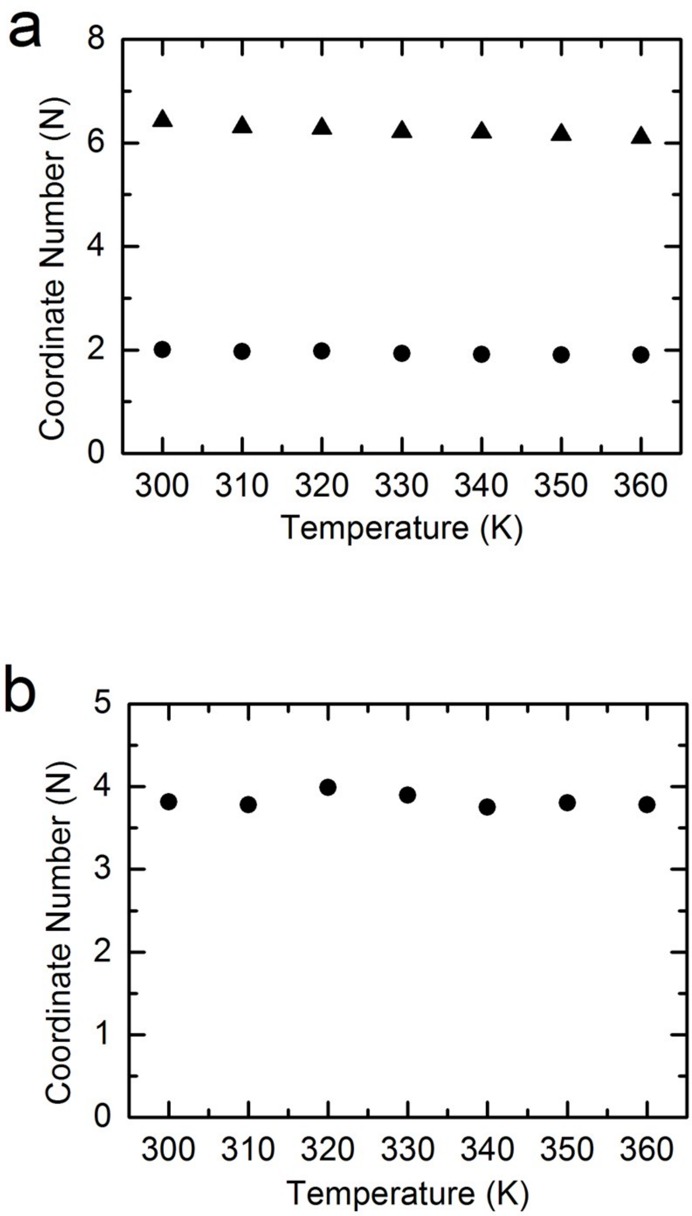

Figure S4. The coordinate number as a function of temperature. (a) HA1-B. The r_{shell} for circle point is 0.5nm, corresponding to the first minimum in the HA1-B g(r); the r_{shell} for triangle point is 0.76nm, corresponding to the second minimum in the HA1-B g(r). (b). CT4-CT4. The r_{shell} is 0.68nm, corresponding to the first minimum in the CT4-CT4 g(r).

We have calculated the coordination number by integrating the radial distribution functions of g(r) as $N = \int_0^{r_{shell}} \rho g(r) 4\pi r^2 dr$, where ρ is the number density and r_{shell} is the minimum in g(r). The results is shown in figure S4. Two different coordinate numbers of HA1-B were calculated by choosing the first minimum 0.5nm and second minimum 0.76nm, corresponding the nearest shell and the next-nearest shell, respectively. The coordination number of the shell retains a relatively stable value such that each HA1 site is surrounded by nearly two anions in the nearest shell. Only the coordinate number for the next-nearest shell decreases slightly from 6.4 to 6.1 with the increasing temperature. The nearest shell represents the strong hydrogen-bond structure between the HA1 and the anions while the next-nearest shell actually stands for the slightly weak hydrogen-bond structures among the HA2, HA3 and the anions. Hence, it means the temperature is almost of no effect on the strong hydrogen-bond structures. The coordinate number for CT4-CT4 also demonstrates that the nearest structure of terminal alkyl chain is almost unchangeable with the increasing temperature.

5. The mean-square displacement and effective diffusion coefficients of atoms from a long 100 ns simulation at 300K.

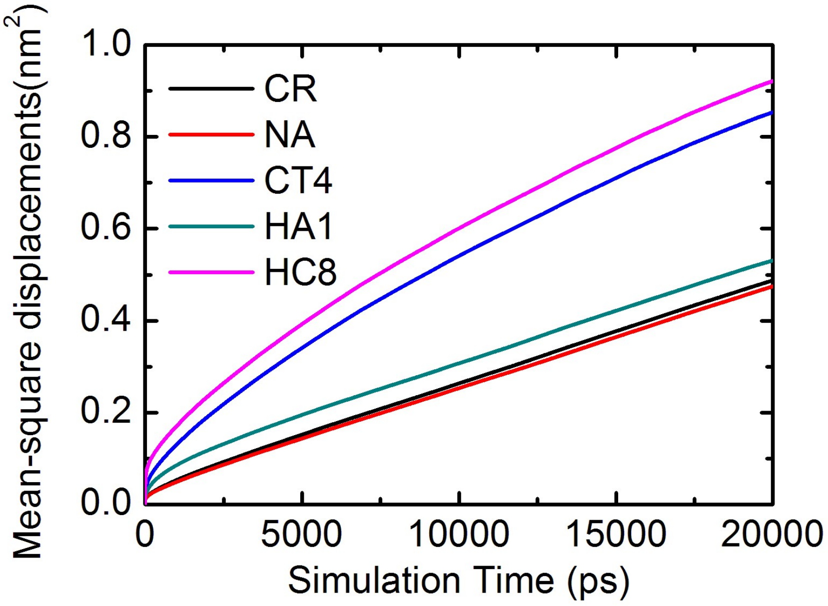

Figure S5. The mean-square displacement of atoms in a 20ns time scale, showing a different steep slope. NA, CR, HA1 atoms belong to imidazoium ring, CT4, HC8 atoms belong to alkyl chain. .

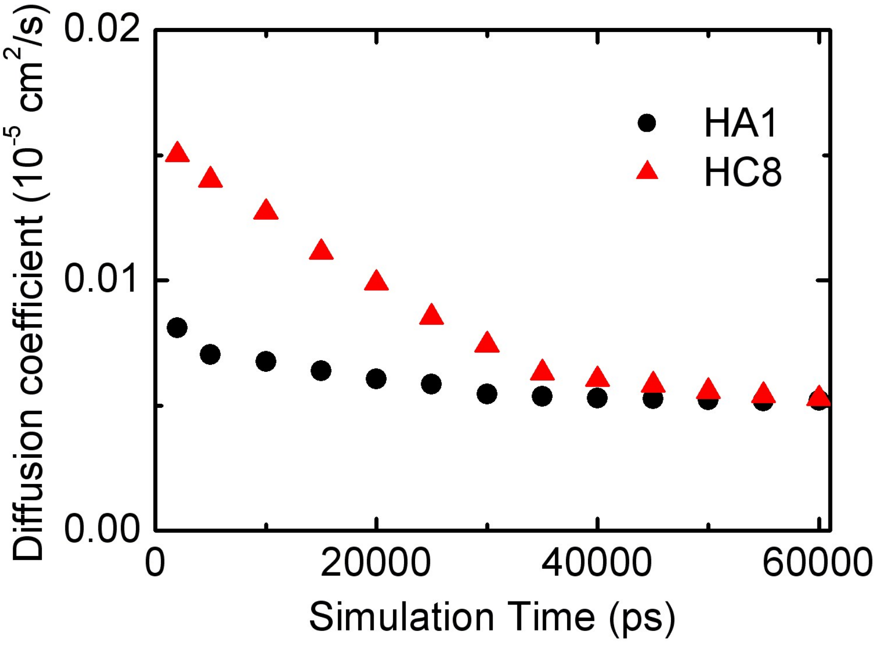

Figure S6. The diffusion coefficients of polar HA1 atom and apolar HC8 atom as a function of simulation time. It is evident that diffusion heterogeneity only exists in a short nanoseconds time scale but finally reverts to homogeneous diffusion behavior.

6. The temperature dependence of diffusion coefficients for cation and anion and the activation energy calculation

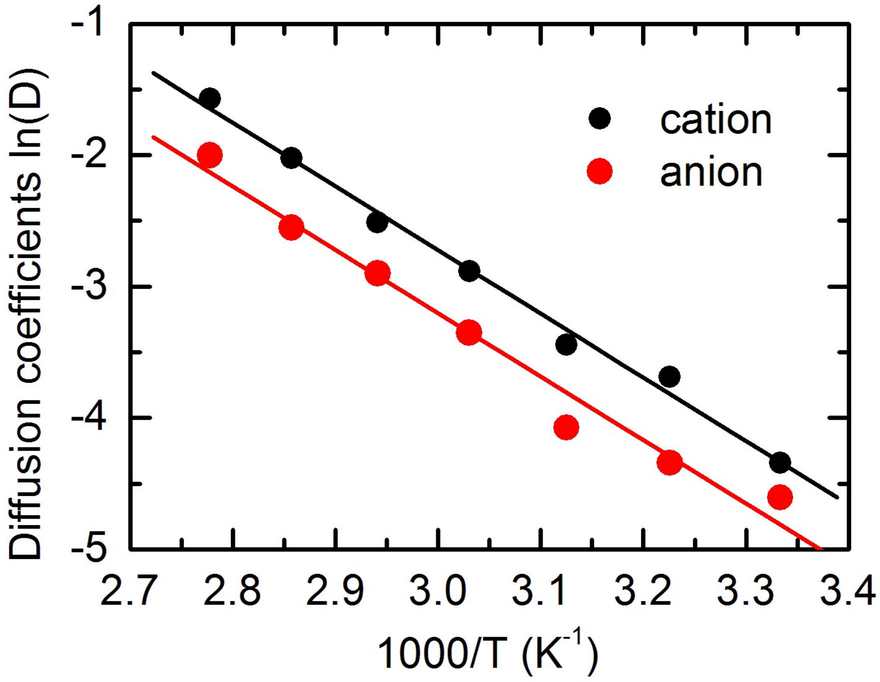

Figure S7. The temperature-dependent diffusion coefficients of cation and anion. The cation and anion were shown in black dots and red dots and fitted by black and red line, respectively.

All of the diffusion coefficient including atoms and ions are calculated in a same method. To ensure the correctness of the diffusion coefficients calculations, we have calculated the mean square displacement in final 10 ns trajectories, and fit it in linear trend after 500 ps, i.e. from the 0.5 ns to 10 ns trajectories to obtain the diffusion coefficient. The activation energy calculation can be obtained by using Arrhenius equation $\mathrm{D} = \mathrm{D}_0 e^{-\frac{E_a}{k_\mathrm{B} T}}$. We can use its logarithmic form, which is $\ln \mathrm{D} = \ln D_0 - \frac{E_a}{k_B T}$. If we use lnD~1/T to draw plot, the slope of the line is $-E_a/k_B$.

7. The hydrogen bonding association dynamics

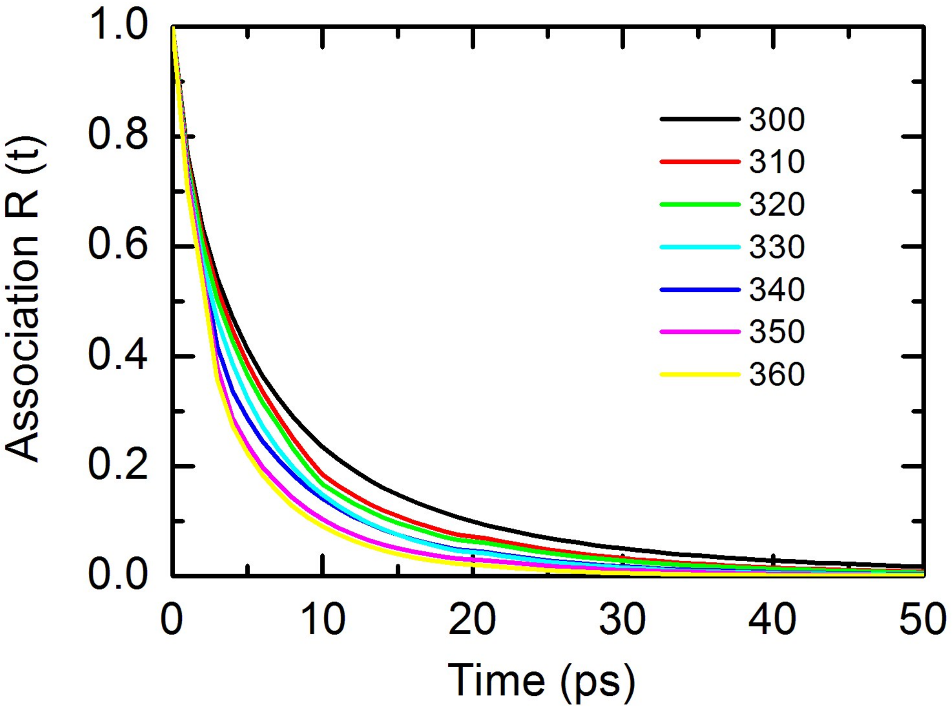

Figure S8. The hydrogen bonding association dynamics between the cation and the anion. The hydrogen bond association was defined as the distance of HA1-F1 within the first coordination shell minimum of RDF of HA1 (imidazolium ring)-F1 (anion).

8. The rotation autocorrelation function of anion

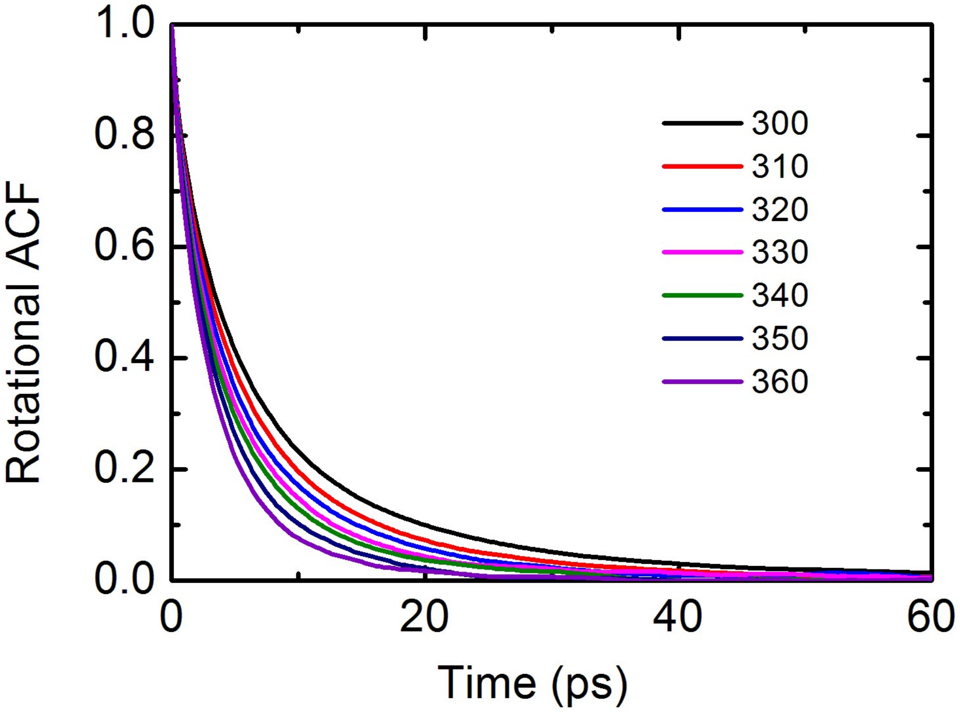

Figure S9. The rotation autocorrelation function of B-F1 direction in anion.

9. References

[1]. H. Tokuda, S. Tsuzuki, M. A. B. H. Susan, K. Hayamizu, M. Watanabe, *J. Phys. Chem. B*, **2006**, *110*, 19593-19600.